Cement and Concrete Research 41 (2011) 1196–1204

Contents lists available at ScienceDirect

Cement and Concrete Research

journal homepage: http://ees.elsevier.com/CEMCON/default.asp

A sorption balance study of water vapour sorption on anhydrous cement minerals and cement constituents

E. Dubina [a], L. Wadsö [b], J. Plank [a,*]

[a] Technische Universität München, Chair for Construction Chemicals, Garching, Lichtenbergstraße 4, 85747, Germany
[b] Lund University, Building Materials LTH, Box 118, 221 00 Lund, Sweden

ARTICLE INFO

Article history:
Received 28 October 2010
Accepted 25 July 2011

Keywords:
Prehydration
Humidity (A)
Clinker (B)
Aging (C)
Sulfate (D)

ABSTRACT

The phenomenon of water vapour sorption by powdered cement constituents exposed to different relative humidities and temperatures was studied. The individual clinker phases C_3S, C_2S, C_3A, C_4AF, calcium sulfates and CaO were tested. Using a water sorption balance, the amount of chemically and physically sorbed water per unit of surface area of the powders and the relative humidity at which water sorption starts to occur on the phases were determined. Various cement clinker phases prehydrate very differently. CaO and C_3A were found to be most reactive towards water vapour whereas the silicates react less. CaO starts to sorb water at very low RHs and binds it chemically. Beginning at 55% RH, orthorhombic C_3A also sorbs significant amounts of water and binds it chemically and physically. Water sorption of C_3S and C_2S only begins at 74% RH, and the amount of water sorbed is minor. Calcium sulfates sorb water predominantly physically.

1. Introduction

The phenomenon of water vapour sorption by cement powders exposed to humidity is known as prehydration of cement. Industrial cements may undergo some prehydration already during the manufacturing process. There, a first contact with water can occur in the mill where clinker is ground together with gypsum at elevated temperature (90–120 °C). Under these conditions, gypsum dehydrates and releases water which can react with the clinker. Furthermore, cement producers sometimes lower the milling temperature by spraying e.g. 2% of water into the mill. Even during storage in the cement silo where temperature may get as high as 70–80 °C, prehydration may proceed due to the continuous release of water from the interground gypsum as long as the temperature exceeds 42 °C [1]. Therefore, cement may already be prehydrated before it is delivered to the customer. Thus, the properties of cement can fluctuate considerably, depending on its history of manufacture and storage.

After delivery and in industrial use, cement may be further stored for several months or even a year before usage. For dry-mix mortars, for example, the usual shelf life is 6 months to 1 year, as stated on the bags. Alteration of the cement properties during storage is highly undesirable, but has been repeatedly noticed by users [2–5]. Such phenomenon may lead to cement failure and is prevalent in climates characterized by relatively high temperature and humidity. The principal consequences of prehydration for the engineering properties of cement are increased setting time, decreased compressive strength and heat of hydration, altered rheological properties and poor response to superplasticizer addition [6–9].

In particular, the surface composition of the individual clinker phases may be affected due to prehydration. Thus, the quality of cement must be assessed based on a profound understanding of the processes occurring during its fabrication and storage. Despite its importance, due to its complex nature and the difficulties associated with the analysis of hydration layers which extend to only a few nanometers in thickness, prehydration of cement is not well understood from the aspect of the interdependency of numerous chemical reactions. Obviously, prehydration of cement is far more complex than the sum of each individual prehydration reaction. Thus, this study on prehydration of pure clinker phases was performed to provide an understanding of the key processes taking place during sorption of water in the complex system of cement.

Ordinary Portland cement (OPC) consists of several clinker phases. The main constituents are variants of: calcium silicates (Ca_3SiO_5 and Ca_2SiO_4), calcium aluminate ($Ca_3Al_2O_6$), and ferrite ($Ca_4Al_{4-x}Fe_xO_{10}$) which are commonly denominated as C_3S, C_2S, C_3A and C_4AF, respectively. Jensen et al. showed that the clinker minerals C_3S, C_2S and C_3A have fundamentally different sensitivities to moisture [10]. For example, C_3A was shown to hydrate at lower relative humidities than either C_3S or C_2S. However, while some factors that govern clinker reactivity towards water vapour such as e. g. the free energy of the mineral's surface are known [11], we still lack in a complete understanding of the mechanisms by which certain cement components are more sensitive to prehydration than others.

* Corresponding author. Tel.: +49 89 289 13151; fax: +49 89 289 13152.
E-mail address: sekretariat@bauchemie.ch.tum.de (J. Plank).

0008-8846/$ – see front matter © 2011 Elsevier Ltd. All rights reserved.
doi:10.1016/j.cemconres.2011.07.009

Table 1
Physicochemical properties of the starting materials.

Material	Source	Purity (wt.%)	Average particle size d_{50} value (μm)
$CaCO_3$	Merck	98.5	14
Al_2O_3	Nabaltec	99.5	20
SiO_2	Euroquarz	99	7
Fe_2O_3	Lanxess	96	3
MgO	Merck	99	4
$NaNO_3$	Merck	99	5

Even more important is the question whether prehydration is solely a reaction between cement and water vapour, or whether it occurs via water vapour condensation, followed by reactions between liquid water and cement. This latter case would entail that prehydration follows the well-known route of dissolution–oversaturation–precipitation in the same manner as during hydration of ordinary cement. Whereas in the first case, a totally different mechanism of prehydration leading to different hydration products may occur.

Generally, water vapour can be sorbed by cement either physically or chemically, or in both ways. Water molecules can physically bind to the surface of cement by van der Waals forces (adsorption), forming mono- and multilayers. At higher relative humidity, capillary condensation and capillary water uptake may occur. Both processes are physical by nature. Additionally, water can react chemically with clinker phases, yielding crystalline hydration products. The chemical incorporation of water into amorphous solids and the formation of early hydration products on the surface of cement particles can result in changes of the properties of cement powder. Generally, physically bound water will be reversibly desorbed when the water vapour pressure is decreased or the temperature is increased. In this case, the forces between the solid (adsorbent) surface and the vapour molecules (adsorbate) are weak. The forces involved in chemical reactions are much greater than those in physical adsorption. Therefore, chemically bound water will not be released by lowering RH to 1% for a short period of time. In this study, physically bound water was defined as water which can be removed by drying at 1% RH for 1 h only, while irreversibly sorbed water was considered to be bound chemically.

In the present work, the physicochemical effects of water sorption on the surfaces of pure clinker phases (monoclinic C_3S, monoclinic β-C_2S, cubic and orthorhombic C_3A and orthorhombic C_4AF) as well as of different sulfates ($CaSO_4$, β-$CaSO_4 \cdot ½H_2O$, $CaSO_4 \cdot 2H_2O$) and of free lime (CaO) were investigated using a water vapour balance instrument. The experiments were conducted to gain an understanding of the principle effects on individual cement constituents.

In this investigation, the RHs at which prehydration of the cement constituents starts to occur, and the amount of water sorbed per unit area of cement component surface were determined. Emphasis was placed on understanding the ratio between physically and chemically sorbed water, and the reversibility of this process. Measurements were conducted at both 20 °C and 40 °C. Finally, the products formed as a result of sample exposure to water vapour were visually investigated by ESEM.

2. Materials and methods

2.1. Materials

Pure cement clinker minerals were prepared by calcination of the respective oxides or carbonates. The characteristics of the starting materials are given in Table 1. From the starting materials, mixtures with molar ratios corresponding to theoretical values were prepared according to Table 2 and homogenized by grinding in a ball mill for about 10 min. Powders were transferred into platinum crucibles and heated to the specific synthesis temperature (Table 2).

C_3S (alite) in monoclinic modification was stabilized by incorporation of 2 wt.% MgO and 1 wt.% Al_2O_3.

The sintering protocol for this phase included a 2 h heating ramp from 100 °C to 1450 °C, then maintaining a constant temperature of 1450 °C for 4 h. Immediately thereafter, the sample was quenched via rapid cooling by removing it from the oven. The sintering process was repeated 3 times until no reflections due to CaO could be observed by X-ray diffraction.

β-C_2S (belite in monoclinic modification) was stabilized by incorporation of 0.5 wt.% B_2O_3. The sintering protocol included 1 h 45 min heating ramp from 100 °C to 1300 °C, then keeping a constant temperature of 1300 °C for 3 h. Subsequently, the sample was quenched in the same manner as for alite. The disappearance of the peaks due to CaO and SiO_2 and progressing formation of β-C_2S was followed via X-ray diffraction.

Preparation of C_3A and C_4AF generally followed the procedures described by Wesselsky et al. [12]. Pure, undoped C_3A and orthorhombic C_3A doped with 4 wt.%Na_2O were prepared. The sintering protocol for cubic C_3A included a 1 h 50 min heating ramp from 100 °C to 1350 °C for the homogenized powders of $CaCO_3$ and Al_2O_3 mixed at stoichiometric ratio (3:1), followed by sintering the sample for 4 h at 1350 °C. Subsequently, the sample was quenched. After the first sintering process, mayenite ($C_{12}A_7$) and free lime were detected as minor byproducts. The sintering process was repeated 3 times to reduce the amount of mayenite and free lime to less than 0.1 wt.% each. For orthorhombic C_3A, $NaNO_3$ was first manually ground in an agate mortar for 10 min; then homogenized with $CaCO_3$ and Al_2O_3 in a ball mill for about 10 min. The homogenized powder was heated for 1 h 50 min from 100 °C to 1350 °C, then sintered at 1350 °C for 3 h and subsequently quenched. The sintering process was repeated several times. After the first burn, the amount of $NaNO_3$ was adjusted depending on the amount of free lime detected by XRD to exclude cubic C_3A as byproduct which can be attributed to the volatility of sodium at high temperatures.

Brownmillerite (C_4AF) was synthesized by sintering an idealized mixture of CaO, Al_2O_3 and Fe_2O_3 at molar ratios of 4:1:1. The oxides were first ground in a ball mill, then heated from 100 °C to 1250 °C

Table 2
Proportions, sintering temperature and periods used for the preparation of 100 g of each clinker phase.

Clinker phase	Amounts in g of							T (°C)/ time (h)[a]
	$CaCO_3$	SiO_2	Al_2O_3	Fe_2O_3	MgO	B_2O_3	$NaNO_3$	
Monoclinic C_3S (alite)	127.1	25.8	1.0	–	2.0	–	–	1450/4 h
Monoclinic β-C_2S (belite)	116.2	34.9	–	–	–	0.5	–	1300/3 h
Cubic C_3A (pure aluminate)	111.1	–	37.7	–	–	–	–	1350/6 h
Orthorhombic C_3A (doped aluminate)	98.1	–	34.5	–	–	–	14.5	1350/3 h
C_4AF (brownmillerite)	82.4	–	21.0	32.9	–	–	–	1250/4 h
CaO (free lime)	178.5	–	–	–	–	–	–	1000/3 h

[a] The sintering process was repeated several times with intermediate grindings to exclude impurities in the form of minor phases.

and finally kept at 1250 °C in an oven for about 4 h. The sample was quenched by rapid cooling. The sintering process was repeated three times until no reflections due to CaO, Al_2O_3 and Fe_2O_3 could be observed by X-ray diffraction.

Free lime was prepared by calcination of $CaCO_3$ over 3 h at 1000 °C.

Grinding of all samples prepared was performed in a ball mill (Planetary Mono Mill PULVERISETTE 6 classic line, Fritsch, Idar-Oberstein, Germany) for 10 min at 250 rpm under air at a temperature of 21 °C and RH of 20%.

As calcium sulfates, gypsum (purity 98 wt.%), β-hemihydrate (purity 97 wt.%) and anhydrite (purity 99 wt.%) from Sigma-Aldrich were used.

Purity of synthesised phases was checked by quantitative X-ray powder diffraction (XRD) using a Bruker D8 Advance X-ray diffractometer (Bruker AXS, Karlsruhe, Germany) with a Bragg–Brentano geometry, equipped with a two-dimensional detector (Vantec-1®, Bruker AXS, Karlsruhe, Germany). The clinker phases were found to be pure within an accuracy of ±1 wt.% for C_2S/C_3S and ±0.5 wt.% for C_3A/C_4AF (Software for Rietveld analysis: Topas 3.0, Bruker AXS, Karlsruhe, Germany).

XRD patterns of all cement components tested in this study are presented in Fig. 1.

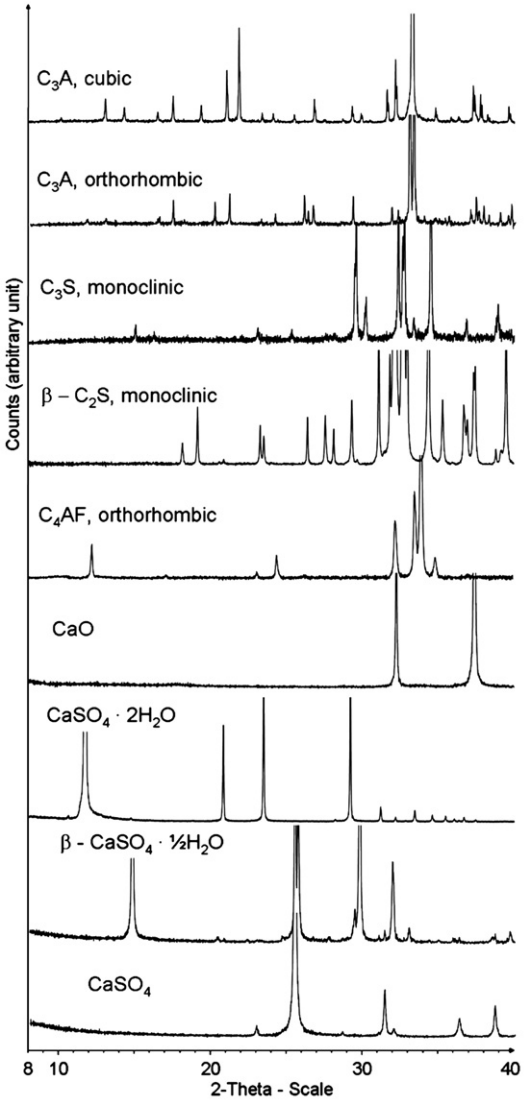

Fig. 1. XRD patterns of clinker phases as prepared and of cement components tested, shown in the range of 8–40° 2 θ.

Table 3
Properties of synthesized pure clinker phases and cement constituents.

Cement constituent	Source	Chemical notation	Average particle size d_{50} value (μm)	Specific surface area (BET) (cm^2/g)
C_3S[a], monoclinic	Self-prepared	Ca_3SiO_5	8.1	5700
C_2S[b], monoclinic	Self-prepared	Ca_2SiO_4	7.4	5500
C_3A, cubic	Self-prepared	$Ca_3Al_2O_6$	6.2	7800
C_3A, orthorhombic[c]	Self-prepared	$Ca_{8,5}NaAl_6O_{18}$	9.0	7100
C_4AF, orthorhombic	Self-prepared	$Ca_4Al_2Fe_2O_{10}$	12.9	2800
CaO	Self-prepared	CaO	4.7	24000
Gypsum	Sigma-Aldrich	$CaSO_4 \cdot 2H_2O$	32.2	7900
Hemihydrate	Sigma-Aldrich	$CaSO_4 \cdot ½H_2O$	10.4	12000
Anhydrite	Sigma-Aldrich	$CaSO_4$	5.9	14000

[a] Doped with 1 wt.% Al_2O_3 and 2 wt.% MgO.
[b] Stabilized with 0.5 wt.% B_2O_3.
[c] Doped with 4 wt.% Na_2O.

The average particle size (d_{50} value) of all phases tested was measured by laser granulometry (Cilas 1064, Cilas, Marcoussis, France). Specific surface area of all samples was determined by N_2 adsorption (BET method) employing a NOVA 4000e surface area analyzer from Quantachrome (Odelzhausen, Germany). The results are presented in Table 3.

2.2. Sorption balance instruments

Two sorption balances (DVS-1000 and DVS Advantage, both from Surface Measurement Systems Ltd., London, UK) were used to measure the moisture uptake of clinker phases, sulfates and CaO. Both sorption balances have similar mode of operation and differ merely in their software. Generally, a sorption balance allows automatic and quantitative measurement of sorption and desorption of water vapour or other gases on small scale samples (5–150 mg) [13]. Sorption balances have been employed successfully to determine the water sorption behaviour and kinetics of materials as diverse as textiles and food preparations [14,15]. The general set-up of a sorption balance is presented in Fig. 2. To conduct the measurement, the sample is placed in a sample pan of the microbalance. Both temperature and relative humidity can be programmed separately. The moisture uptake by the sample is measured while it is exposed to a nitrogen flow with a well defined RH of ±1%. RH is controlled by mixing dry and water vapour saturated nitrogen gas. The relative humidity can be changed either in steps or in ramps, and it can be increased or decreased. The microbalance has a resolution of 0.1 μg. In our experiments, nitrogen was supplied from a Nitrogen generator (G2, Domnick Hunter Ltd, Gateshead, England).

2.3. Experimental program for water vapour sorption

The moisture uptake can be investigated by different relative humidity programs constructed from RH-steps and RH-ramps [16,17]. In the present study, both ramp and step programs to investigate different aspects of the moisture uptake process were used. In all cases, the temperature was held constant at 20 °C or 40 °C during each measurement.

Fig. 3 shows the ramp program used in our study. There, RH is continuously increased from 1% to 95% RH at a constant rate of about 0.16% RH per minute. It is important to stabilise the sample for 1 h at 1% RH

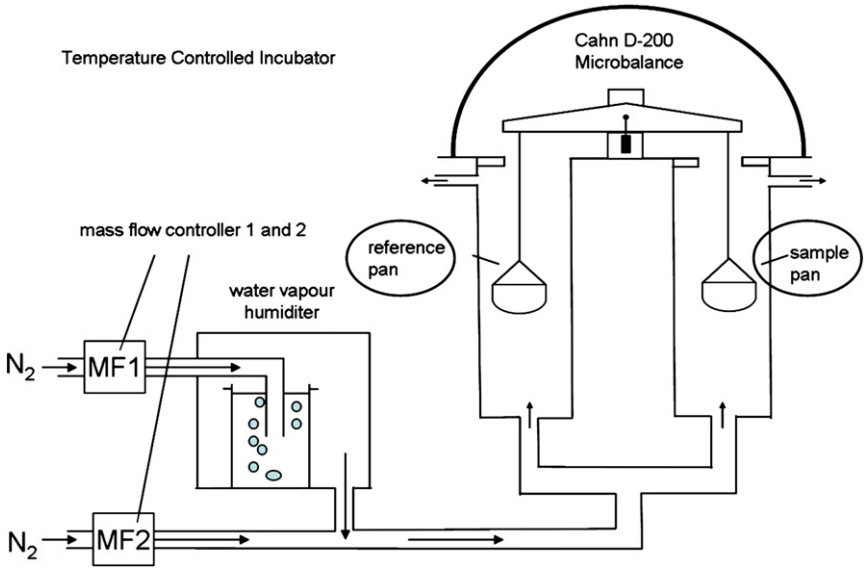

Fig. 2. Schematic illustration of a DVS instrument.

before increasing the relative humidity. Furthermore, at the end of the exposure to water vapour, each sample was subjected to 1%RH to distinguish between physically and chemically bound water. Whereas, with the ramp program it is possible to obtain a mass change profile for the sample. This makes it possible to assess the threshold value of RH (onset point) at which a sample starts to sorb water.

Fig. 4 shows the step and down program for relative humidities of between 60% and 95%. In this program, RH is increased from 1% to the desired RH, and then decreased again to 1% RH. This program makes it possible to distinguish between physically and chemically bound water. The physically bound water can be removed by drying at 1%RH (reversible process); while the chemically bound water cannot be removed from the surface after reaction with water vapour (irreversible process). All experiments in this mode were performed at high RHs between 60% and 95%. For calculation of the reversibly and irreversibly bound mass of water (w), the following formula was used:

$$w = \frac{m(\varphi)_i - m_o}{m_o} \quad (1)$$

where φ is the relative humidity, $m(\varphi)_i$ is the mass of the sample after water vapour sorption, and m_0 is the initial dry mass of the sample. All experiments with the program in step and down mode were done at both 20 °C and 40 °C to determine the temperature influence on the water vapour uptake. The limitation of this method is that it requires samples to achieve the sorption–desorption equilibrium within 1 h. This may or may not be the case with the samples tested here, and establishment of equilibrium conditions was not checked here. A further problem in the interpretation of the data may relate to the potential presence of induction period phenomena occurring in the reactive processes involved here [11]. Therefore, values obtained according to this method should be interpreted as qualitative, and not be taken as quantitative and final.

2.4. SEM imaging

Scanning electron microscopy (SEM) images were obtained from a FEI XL 30 FEG microscope equipped with a large field detector under low vacuum conditions (1 mbar H_2O pressure, corresponding to ~4% RH at room temperature). Observations on the morphology of the products

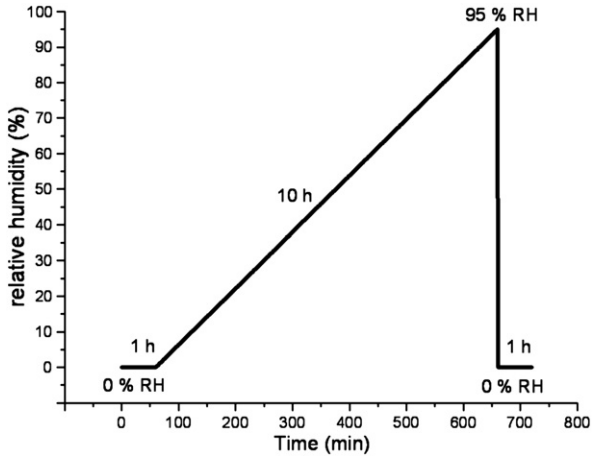

Fig. 3. Development of relative humidity over time used in the ramp program.

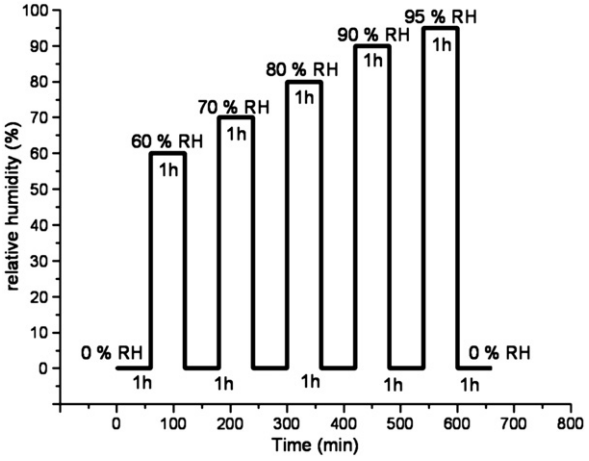

Fig. 4. Relative humidity program used in the step and down mode.

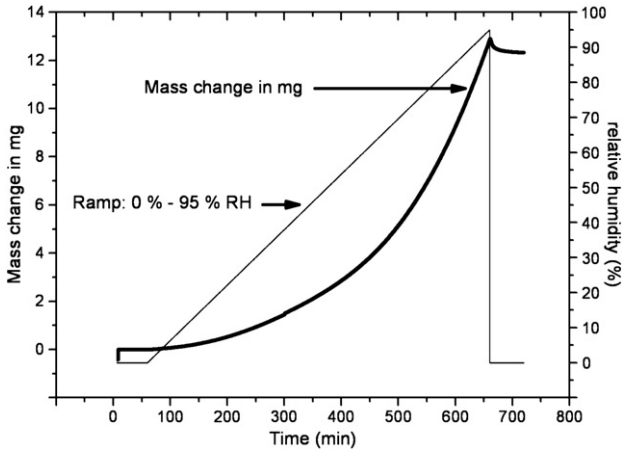

Fig. 5. Water vapour sorption of CaO, determined on a sorption balance at 20 °C using the ramp mode and measured over a period of 11 h (initial mass of sample: 90.2192 mg).

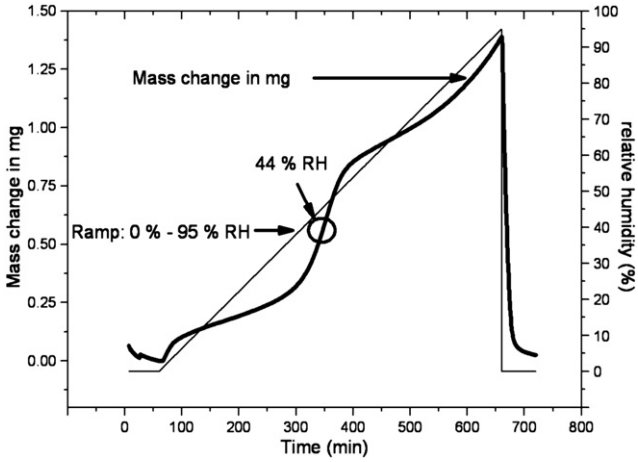

Fig. 7. Water vapour sorption of β-$CaSO_4 \cdot ½H_2O$, measured on a sorption balance at 20 °C, using ramp mode, measured over a period of 11 h (initial mass of sample: 74.9417 mg).

were performed on uncoated samples before and after exposure to relative humidity after storage in the sorption balance instrument.

3. Results and discussion

3.1. Total water sorption

The cement constituents tested showed significantly different mass change profiles in the range between 1% and 95% RH. Generally, three different behaviours were observed.

First, CaO (free lime) already starts to sorb water at very low relative humidity (<10% RH). Its uptake of water increases exponentially with RH. Fig. 5 shows the mass change profile of CaO using the ramp program. The CaO sample investigated sorbed a total of 0.14 mg of water per mg CaO over a period of 11 h. This amount corresponds to ~40% conversion of CaO to portlandite $Ca(OH)_2$. Obviously, free lime strongly attracts water vapour and possibly acts as a drying agent (desiccant) in cement. When in the final part of the experiment humidity was decreased from 95% to 1% RH, not much desorption of water did occur.

Thus, it confirms that almost all of the water sorbed by CaO is irreversibly (chemically) bound.

Second, some clinker minerals such as C_3A or C_4AF exhibit a very minor uptake of water until a specific threshold RH value is exceeded. This point – "the threshold point" or on-set – varies with type of clinker phase, temperature and specific surface area of the individual phase. Fig. 6 shows as an example the mass change profile for cubic C_3A. Beginning at 80% RH, cubic C_3A starts to take up a noticeable amount of water vapour. In this experiment, C_3A sorbed ~0.9 wt.% of water, based on the dry mass of C_3A. From this value, 0.7 wt.% was not removable and thus bound by chemical reaction of C_3A.

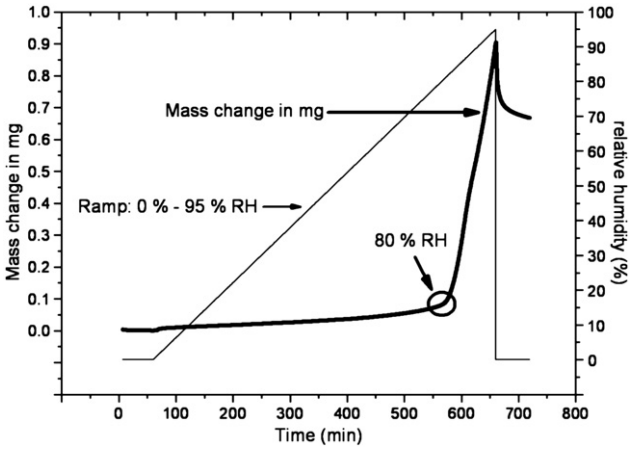

Fig. 6. Water vapour sorption of cubic C_3A, determined on a sorption balance at 20 °C using ramp mode and measured over a period of 11 h (initial mass of sample: 97.3439 mg).

The third category is represented by the sulfates. At increasing humidity, they exhibit a characteristic, step-wise uptake of water. Fig. 7 displays a typical mass change diagram for β-$CaSO_4 \cdot ½H_2O$. Its mass change profile developed in the ramp mode shows an on-set point for water sorption at around 34% RH and several inflexion points, the most significant one at 44% RH. This behaviour can be interpreted such that at ~34% RH, rapid hydration of β-hemihydrate begins until it slows down at RH values beyond 60%.

Table 4 summarizes the RH values of the on-set point for water uptake (i.e. the RHs at which water sorption starts to occur) for all cement constituents tested as obtained from the mass change profiles.

3.2. Distinction between chemically and physically sorbed water

The amount of chemically and physically bound water can be differentiated by studying water sorption using the step mode. Tests performed at RHs between 60% and 95% again showed different types of water vapour sorption behavior by the cement constituents tested.

Three different kinds of water uptake were observed:

(a) Water vapour is mostly sorbed chemically; the water is bound irreversibly to the phase and cannot be removed by drying for 1 h at 1% RH and 20 °C. An example for this behaviour is free lime (see Fig. 8).
(b) Water vapour is sorbed both chemically and physically; the physically sorbed part of water can be removed by drying at 1%

Table 4
Relative humidities at which cement constituents start to take up water vapour, measured on a sorption balance at 20 °C using the ramp mode.

Cement constituents	Relative humidity at which water sorption starts (%)
CaO	<10
$CaSO_4 \cdot 2H_2O$	24
β-$CaSO_4 \cdot ½H_2O$	34
C_3A, orthorhombic	55
$CaSO_4$	58
C_2S, monoclinic	64
C_3S, monoclinic	63
C_4AF, orthorhombic	78
Pure C_3A, cubic	80

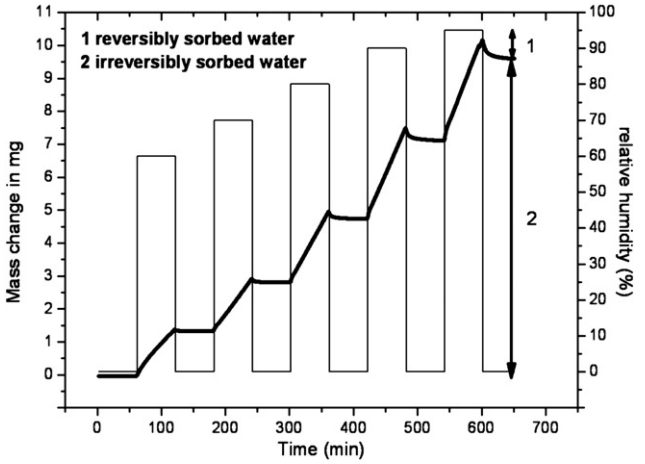

Fig. 8. Determination of physically (1) and chemically (2) sorbed water on CaO, measured on a DVS instrument at 20 °C using step and down mode (initial mass of sample was: 58.5219 mg).

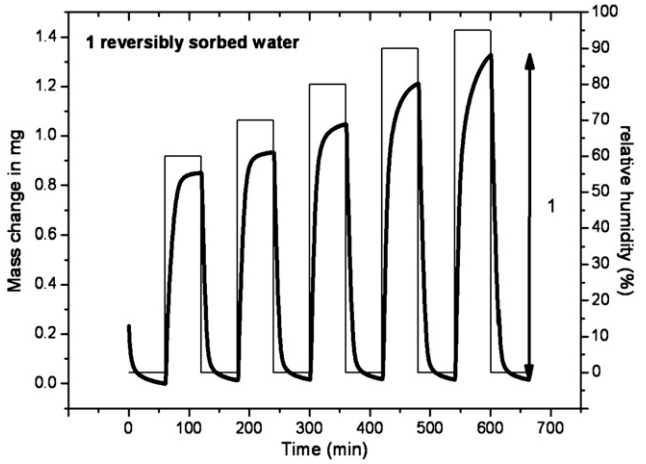

Fig. 10. Determination of physically (1) sorbed water on β-$CaSO_4 \cdot ½H_2O$, measured on a DVS instrument at 20 °C using step and down mode (initial mass of sample: 68.4202 mg).

RH; whereas, the chemically sorbed part cannot be removed by drying. This behaviour is represented by cubic C_3A (see Fig. 9).

(c) Water vapour is mostly sorbed physically and can be removed almost completely by drying at 1% RH. Such behaviour is exemplified by β-$CaSO_4 \cdot ½H_2O$ (see Fig. 10).

Free lime sorbs all water vapour irreversibly and reacts to form portlandite. Only at very high RHs (around 90–95%), a small amount of physically bound water can be removed. This pronounced ability of CaO to sorb water vapour very quickly and irreversibly can possibly reduce or even prevent prehydration of other constituents when cement is exposed to moisture during storage. Thus, cements exhibiting a relatively high content of free lime possibly sorb more water than cements possessing a low amount of free lime. Cubic C_3A, on the other hand, is an example of a cement constituent which shows both physical and chemical sorption. Its chemical sorption leads to the formation of C-A-H phases.

For β-$CaSO_4 \cdot ½H_2O$, most of the water vapour uptake is reversible, and thus can be removed by drying at 1% RH. This result is unexpected, because β-$CaSO_4 \cdot ½H_2O$ is known to react almost instantaneously with liquid water to form gypsum. For this reason, it is commonly applied with set retarders to achieve practical setting times in building products. However, this reaction normally occurs via the dissolution–oversaturation–precipitation mechanism. Here, β-$CaSO_4 \cdot ½H_2O$ obviously does not dissolve and react, but sorbs water molecules only physically.

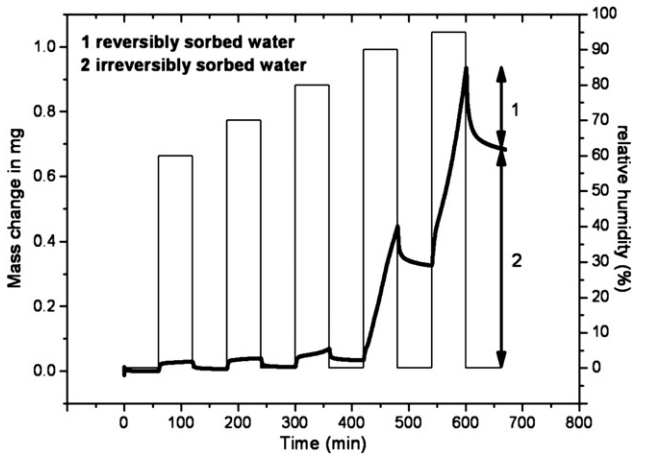

Fig. 9. Determination of physically (1) and chemically (2) sorbed water on cubic C_3A, measured on a DVS instrument at 20 °C using step and down mode (initial mass of sample: 58.8794 mg).

Table 5 presents a summary on the water sorption measured for all samples tested by using the two different methods (ramp and step and down mode). There, the amount of water sorbed by each cement constituent tested at 20 °C over a period of 11 h is presented as wt.% of original mass of sample and as mass per unit of specific surface area of sample. It becomes obvious that free lime and – to less extent – doped orthorhombic C_3A sorb the highest amount of water, followed by the calcium sulfates. Whereas, the silicates show only a minor uptake of water.

Because water vapour sorption first and above all is a surface process, the uptake of water by a surface is directly linked to its granular size which is expressed by its specific surface area. To account for this, the amount of water sorbed per unit area was calculated using the values for the specific surface area (BET method) of the fresh, non-prehydrated samples as shown in Table 3. Additionally, it was found that the BET surface area of the fresh samples did not change much as a result of water sorption. Thus, the values shown in Table 5 represent the amount of water sorbed per unit of surface area of the non-prehydrated sample. Generally, the relative order of the samples was found to be independent of the test mode. Fig. 11 shows a comparison of relative water uptake per specific surface area for different cement constituents tested. There, it becomes obvious that free lime and doped, orthorhombic C_3A by far sorb the highest amounts of water per surface area (~50–60 $\cdot 10^{-7}$ g/cm^2). This is followed at some distance by β-$CaSO_4 \cdot ½H_2O$

Table 5
Total mass changes of cement constituents obtained from DVS measurements for two different modes of exposure to humidity.

Cement constituent	Mass change after exposure to max. 95% relative humidity at 20 °C			
	Ramp method		Step and down method	
	(wt.%)	$\left(\frac{10^{-7}\text{g}}{\text{cm}^2}\right)$	(wt.%)	$\left(\frac{10^{-7}\text{g}}{\text{cm}^2}\right)$
CaO	14.24	59.3	17.35	72.3
C_3A, orthorhombic	3.62	51.0	5.29	74.5
$CaSO_4 \cdot ½H_2O$	1.85	15.4	1.94	16.2
C_4AF, orthorhombic	0.40	14.3	0.37	13.2
C_3A, cubic	0.92	11.8	1.57	20.1
$CaSO_4$	1.03	7.4	1.01	7.2
$CaSO_4 \cdot 2H_2O$	0.40	5.1	0.36	4.6
C_3S, monoclinic	0.09	1.6	0.08	1.4
C_2S, monoclinic	0.09	1.6	0.04	0.7

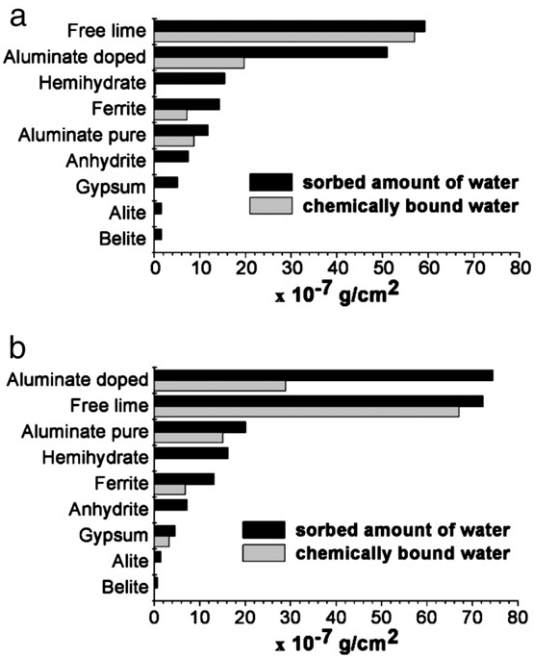

Fig. 11. Comparison of relative water uptake per unit of specific surface area for different cement constituents tested in a) ramp mode and b) step and down mode.

(~$15\cdot10^{-7}$ g/cm^2), C_4AF (~$14\cdot10^{-7}$ g/cm^2) and undoped, cubic C_3A (~$12\cdot10^{-7}$ g/cm^2). While the silicates sorb a surprisingly low amount of water (~$1.6\cdot10^{-7}$ g/cm^2). Taking into account that the density of sorbed water is roughly 1 g/cm^3 we can estimate the equivalent thicknesses of the water layers sorbed on the surfaces of CaO and C_3S as ~60 nm and 1.6 nm, respectively.

This result instigates that in some cases such as for the silicates, prehydration entails only a very minor portion of the bulk substance. In this case, an ultra-thin layer of only few nanometer thickness is being formed. Still, these small amounts of sorbed water can affect the chemical and engineering properties of the calcium silicates, causing for example retardation of hydration and decreased early strength [9]. While for other cement constituents, prehydration probes much deeper into the bulk material and affects a large portion of it. A representative example for this behaviour is free lime where a significant portion of the bulk material is chemically converted to portlandite.

3.3. ESEM imaging

Fig. 12 shows ESEM images of fresh, anhydrous cubic C_3A and of the same sample prehydrated with water vapour at 20 °C in the step and down program. The specimen exposed to water vapour exhibits numerous platelets of C-A-H phases whereas the surface of the anhydrous C_3A is free of them.

Additional ESEM images of both fresh and prehydrated β-$CaSO_4\cdot½H_2O$ are in perfect agreement with the results obtained from sorption balance measurements. No changes on the surface of the binder were detected after prehydration (Fig. 13).

3.4. Effect of temperature on water vapour sorption

For all samples, the moisture capacity profiles were also measured at 40 °C in the step and down mode to elucidate the effect of temperature on water vapour sorption. Comparison of the sorption profiles obtained at 20 °C and 40 °C, respectively, indicates that increased temperature shifts the on-set point where uptake of water begins to lower RHs. The strongest effect of increased temperature was observed for pure C_3A (Fig. 14). Additionally, increasing the

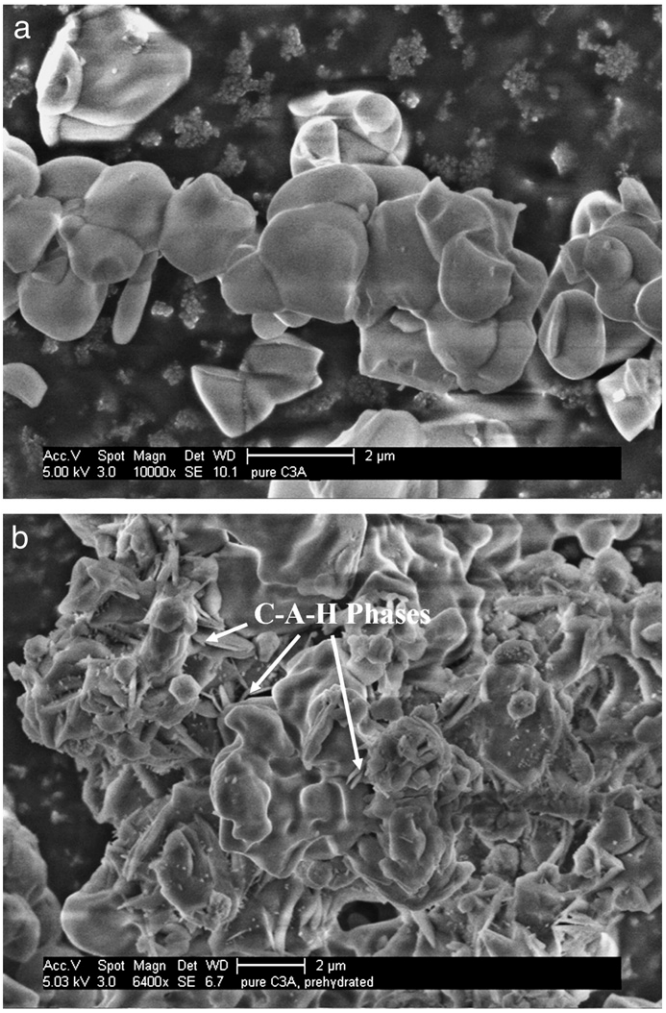

Fig. 12. ESEM images of cubic C_3A: a) fresh, anhydrous; b) prehydrated over 5 h at 60–95% RH and subsequently dried at 1% RH for 1 h at 20 °C.

temperature also led to a significantly higher water uptake. For C_3A, at 40 °C and 80% RH, the total amount of sorbed water is ~5 times higher than that at 20 °C. At both temperatures, the amount of water chemically bound by C_3A generally increases when RH exceeds 80% RH. This phenomenon is explained by the different values of absolute humidity existing in the gas phase at different temperatures. Generally, the water vapour pressure at saturation is a function of temperature. Consequently, the absolute water content occurring at a constant RH increases with temperature. At any RH, at 40 °C there is about three times more water vapour present in the atmosphere than at 20 °C. This higher concentration of water increases the rate of water sorption and results in faster achievement of the sorption equilibrium.

For CaO, increased temperature accelerated water sorption so much that already between 60% and 70% RH, most of the CaO was completely hydrated (Fig. 15). Sorption by CaO was largely irreversible and occurred at a significantly higher rate at 40 °C. Obviously, the rate of reaction with water inside the CaO particles is significantly increased by higher temperature. As a rule of thumb, chemical reactions double their kinetics every 10 K, so the increase observed for CaO is to be expected. At 40 °C and 80% RH, still a small amount of physically, reversibly bound water was found for CaO. This instigates that at this stage, CaO is almost completely converted to $Ca(OH)_2$ which can sorb water only via physical sorption. This amount is removed by drying at 1% RH.

Opposite to CaO, for some cement constituents, an increase of temperature only slightly affected their water sorption. For example,

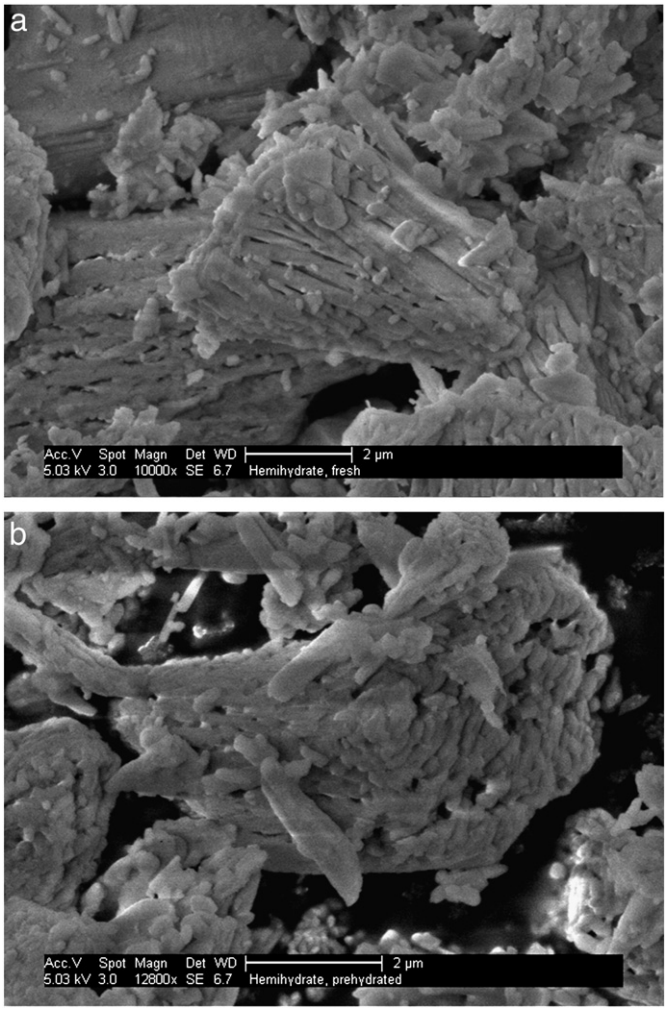

Fig. 13. ESEM images of β-$CaSO_4 \cdot ½H_2O$: a) fresh; b) prehydrated at 20 °C over 5 h at 60–95% RH and subsequently dried at 1% RH for 1 h.

at 40 °C β-$CaSO_4 \cdot ½H_2O$ does not show a significant increase in the total amount of sorbed water (Fig. 16). This behavior instigates that this phase sorbs water only through physical sorption which is quite independent of temperature.

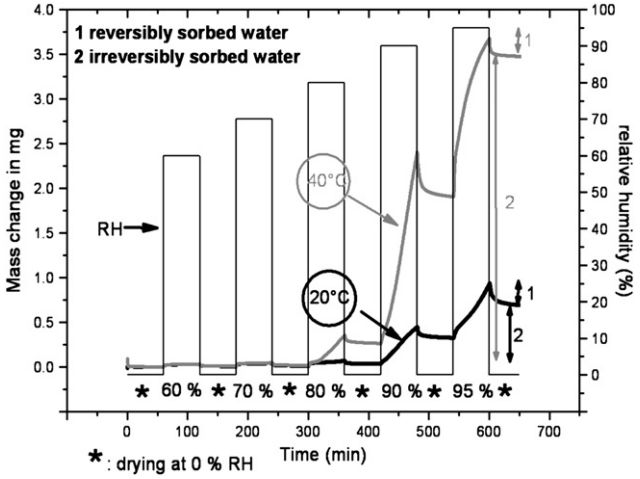

Fig. 14. Water vapour sorption isotherms for pure C_3A, measured at 20 °C and 40 °C, respectively, in step and down mode (initial masses of samples: m (20 °C) = 58.8794 mg, m (40 °C) = 56.2018 mg).

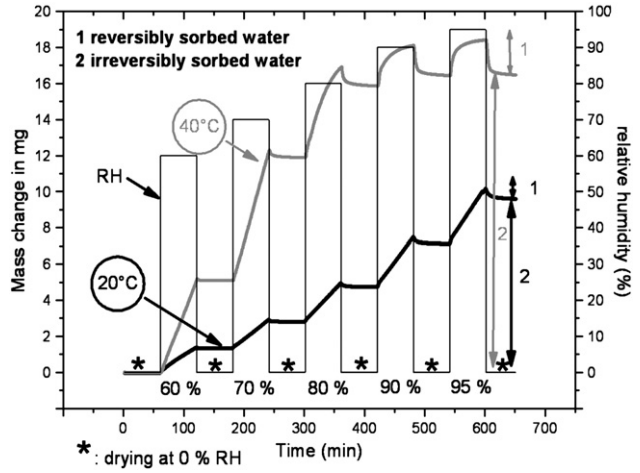

Fig. 15. Water vapour sorption isotherms for CaO measured at 20 °C and 40 °C, respectively, in step and down mode (initial masses of samples: m (20 °C) = 58.5219 mg; m (40 °C) = 53.005 mg).

Finally, Table 6 gives a comparison of the total amounts of water sorbed at 20 °C and 40 °C, respectively, for all samples tested. The values in the table present the amount of water sorbed in percentage, milligram and per unit of specific surface area (BET method). The results show that increased temperature which results in an increased amount of water content in the gas phase affects the samples quite differently. Some cement constituents, e. g. C_3A and CaO, sorb more water at 40 °C whereas others (e. g. β-$CaSO_4 \cdot ½H_2O$) respond less to an increase in temperature, because they only show physical adsorption which is more rapid.

4. Conclusions

This study demonstrated that a dynamic vapour sorption balance is a very useful instrument to investigate the interaction between gaseous water and cement constituents. The sorption of water vapour on pure clinker phases, calcium sulfates and CaO was studied at different RHs and temperatures using ramp and step and down programs for adjusting RH. Investigation via ESEM complemented and confirmed the results obtained with the sorption balance instrument. From the aforementioned results of this study, the following conclusions could be obtained:

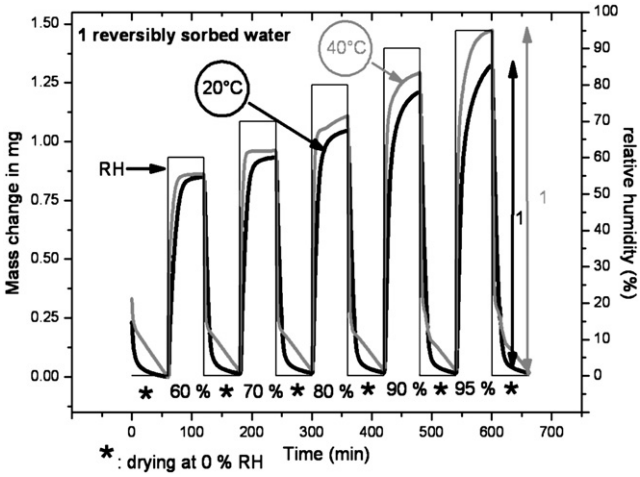

Fig. 16. Water vapour sorption isotherms for β-$CaSO_4 \cdot ½H_2O$ measured at 20 °C and 40 °C, respectively, in step and down mode (initial masses of samples: m (20 °C) = 68.4202 mg; m (40 °C) = 59.3159 mg).

Table 6
Comparison of mass changes for samples tested at 20 °C and 40 °C, respectively, in step and down mode.

Cement constituent	Mass change after exposure to humidity					
	T = 20 °C			T = 40 °C		
	(wt.%)	(mg)	$\left(\frac{10^{-7}g}{cm^2}\right)$	(wt.%)	(mg)	$\left(\frac{10^{-7}g}{cm^2}\right)$
C_3A, orthorhombic	5.29	3.45	74.5	13.55	11.22	190.8
CaO	17.35	10.10	72.3	34.75	18.42	144.8
C_3A, cubic	1.57	0.93	20.1	6.53	3.67	83.7
β-$CaSO_4 \cdot ½H_2O$	1.94	1.32	16.2	2.48	1.47	20.7
C_4AF, orthorhombic	0.37	0.27	13.2	0.99	0.91	35.4
$CaSO_4$	1.01	0.93	7.2	1.52	3.06	10.9
$CaSO_4 \cdot 2H_2O$	0.36	0.21	4.6	0.85	0.42	10.8
C_3S, monoclinic	0.08	0.07	1.4	0.24	0.18	4.2
C_2S, monoclinic	0.04	0.01	0.7	0.17	0.18	3.1

Cement constituents show fundamentally different onset points at which water uptake starts to occur. The amount of sorbed water per specific surface was differentiated for each cement constituent. It showed that sorbed water can be bound physically, chemically or in both ways. The experiments demonstrated that both free lime and orthorhombic C_3A sorb large amounts of water. They are followed by β-$CaSO_4 \cdot ½H_2O$ and cubic C_3A. C_4AF, gypsum and anhydrite sorb very low amounts of water, whilst the silicates C_3S and C_2S sorb almost no water at all.

A comparison of the sorption isotherms at 20 °C and 40 °C indicates that for all clinker phases, increasing temperature causes moisture uptake to occur at lower RHs. Obviously, different cement constituents exhibit very different behaviour towards water vapour at high temperature.

The subject of prehydration of cement is highly interesting for cement manufacturers and applicators. Therefore several questions on this phenomenon should be clarified in further investigations. For example, the impact of water vapour on the behaviour of binary mixtures, with a focus on C_3A mixed with different calcium sulphates, should be studied in more detail. Such experiment may give an answer to the question whether the mechanism behind prehydration is solely based on a topochemical reaction between cement and water vapour, or whether it entails a reaction with liquid condensed water which follows the well known route of cement hydration characterized by a dissolution–oversaturation–precipitation process.

Furthermore, prehydration of pure clinker phases and other cement constituents should be studied in presence of CO_2 to understand the synergistic impact of CO_2 and water vapour on the ageing of cement.

Acknowledgments

The authors are grateful to Nanocem (Core Project # 7) for the financial support of this work. Additionally, the authors like to thank Leon Black, University of Leeds/U.K and Holger König, HeidelbergCement, Leimen/ Germany for their input in many discussions.

References

[1] A.E. Mould, D.W. Williams, The effects of high ambient temperatures on gypsum plasters, Build. Sci. 9 (1974) 243–245.
[2] C. Maltese, C. Pistolesi, A. Bravo, F. Cella, T. Cerulli, D. Salvione, Effect of moisture on the setting behavior of Portland cement reacting with an alkali-free accelerator, Cem. Concr. Res. 37 (2007) 856–865.
[3] G. Schmidt, T.A. Bier, K. Wutz, M. Maier, Characterization of the ageing behavior and its effect on their workability properties, ZKG Int. 60 (6) (2007) 94–103.
[4] C.-S. Deng, C. Breen, J. Yarwood, S. Habesch, J. Phipps, B. Caster, G. Maitland, Ageing of oilfield cement at high humidity: a combined FEG-ESEM and Raman microscopic investigation, J. Mater. Chem. 12 (2002) 3105–3112.
[5] F. Winnefeld, Influence of cement ageing and addition time on the performance of superplasticizer, ZKG Int. 61 (11) (2008) 68–77.
[6] V.S. Sprung, Effect of storage conditions on the properties of cements, ZKG Int. 30 (6) (1978) 305–309.
[7] K. Theisen, V. Johansen, Prehydration and strength development of Portland cement, J. Am. Ceram. Soc. Bull. 54 (9) (1975) 787–791.
[8] L. Barbic, V. Tinta, B. Lozar, V. Marinkovic, Effect of storage time on the rheological behavior of oil well cement slurries, J. Am. Ceram. Soc. 74 (5) (1991) 945–949.
[9] E. Dubina, L. Black, R. Sieber, J. Plank, Interaction of water vapour with anhydrous cement minerals, Adv. Appl. Ceram. 109 (5) (2010) 260–268.
[10] O.M. Jensen, P. Hansen, E.E. Lachowski, F.P. Glasser, Clinker mineral hydration at reduced relative humidities, Cem. Concr. Res. 29 (1999) 1505–1512.
[11] O.M. Jensen, Thermodynamic limitation of self-desiccation, Cem. Concr. Res. 25 (1995) 157–164.
[12] A. Wesselsky, O.M. Jensen, Synthesis of pure Portland cement phases, Cem. Concr. Res. 39 (2009) 973–980.
[13] A. Anderberg, L. Wadsö, Method for simultaneous determination of sorption isotherms and diffusivity of cement-based materials, Cem. Concr. Res. 38 (2008) 89–94.
[14] D. Enke, M. Rückriem, A. Schreiber, J. Adolphs, Water vapour sorption on hydrophilic and hydrophobic nanoporous materials, Appl. Surf. Sci. 256 (2010) 5482–5485.
[15] Ch.C.W. Spackman, Sh.J. Schmidt, Characterising the physical state and textural stability of sugar gum pastes, Food Chem. 119 (2010) 490–499.
[16] L. Wadsö, N. Markova, Comparison of three methods to find the vapour activity of a hydration step, Eur. J. Pharm. Biopharm. 51 (2001) 77–81.
[17] L. Wadsö, A. Anderberg, I. Åslund, O. Söderman, An improved method to validate the relative humidity generation in sorption balances, Eur. J. Pharm. Biopharm. 72 (2009) 99–104.